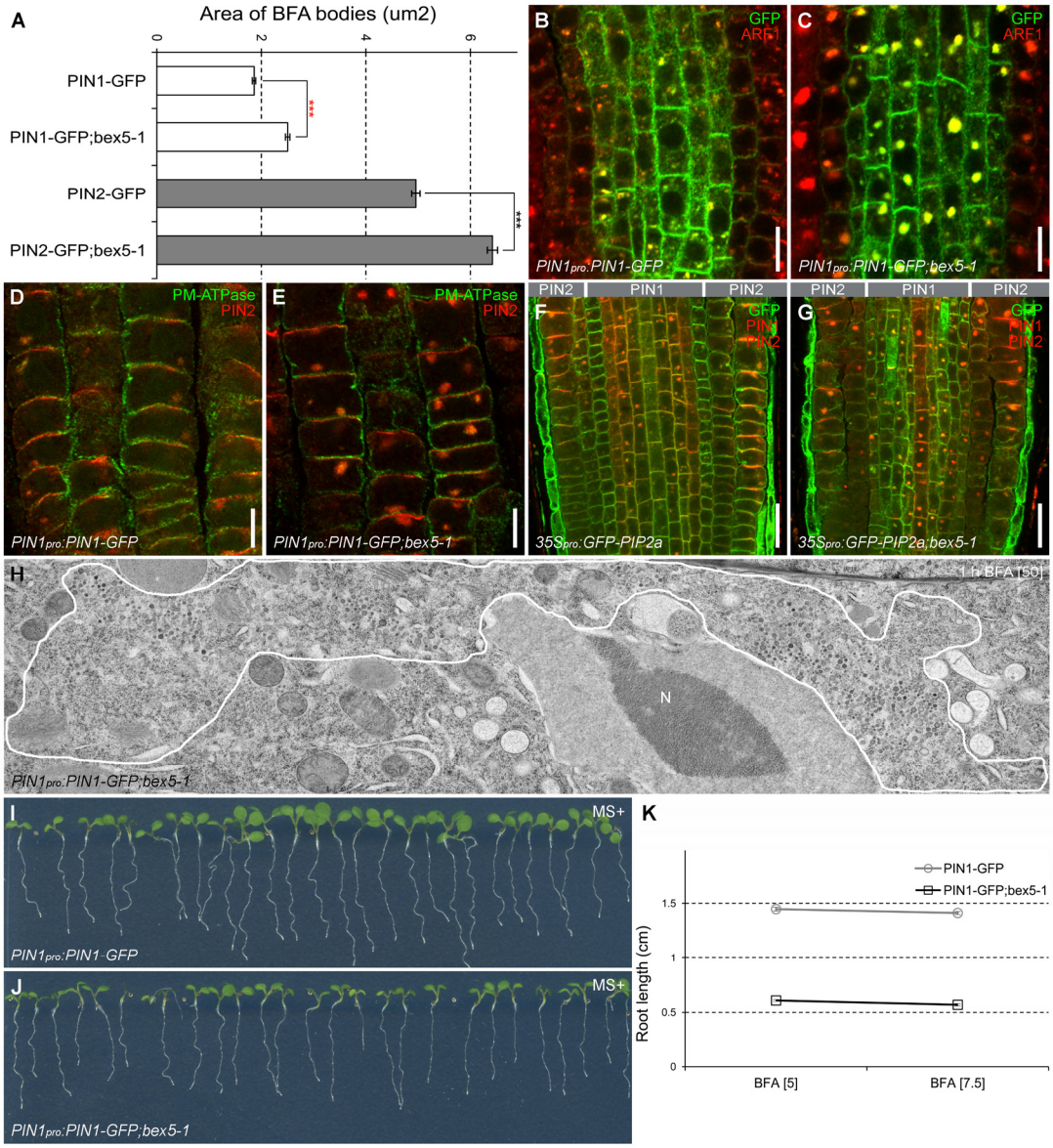

Supplemental Figure 1. *bex5* Shows Enhanced Sensitivity to BFA.

(A) to **(G)** The *bex5-1* mutation causes protein hyper-accumulation into BFA bodies. PIN1-GFP and PIN2-GFP accumulate in larger BFA bodies in the *bex5-1* mutant treated for 1.5-h with 25 µM BFA (n = 150 BFA bodies from 10 roots; red stars, t-test p-value = 1.33E-26; black stars, t-test p-value = 1.15E-25) **(A)**. Immunolocalization of PIN1-GFP and ARF1 (**[B]** and **[C]**), PM-ATPase and PIN2 (**[D]** and **[E]**) or GFP-PIP2a, PIN1, and PIN2 (**[F]** and **[G]**) in BFA-treated (1.5-h; 25 µM) controls (**[B]**, **[D]** and **[F]**) and *bex5-1* (**[C]**, **[E]** and **[G]**) roots show defective protein accumulation in enlarged BFA bodies in *bex5-1*.

(H) BFA-induced agglomerations have abnormal morphology in the *bex5-1* mutant. They are spread over large areas of the cell (white border), are less compact and the vesicles themselves have an impaired morphology. Seedlings were treated for 1 sh with 50 µM BFA.

(I) and **(J)** 5-day-old $PIN1_{pro}$*:PIN1-GFP;bex5-1* seedlings **(J)** are smaller than $PIN1_{pro}$*:PIN1-GFP* **(I)**.

(K) Evaluation of root length of 7-day-old $PIN1_{pro}$*:PIN1-GFP* and $PIN1_{pro}$*:PIN1-GFP;bex5-1* seedlings grown on 5 µM and 7.5 µM BFA (n = 128).

N, Nucleus. Scale bars are 10 µm **(B)** to **(E)**, 20 µm **(F)** and **(G)**. Error bars represent SE.

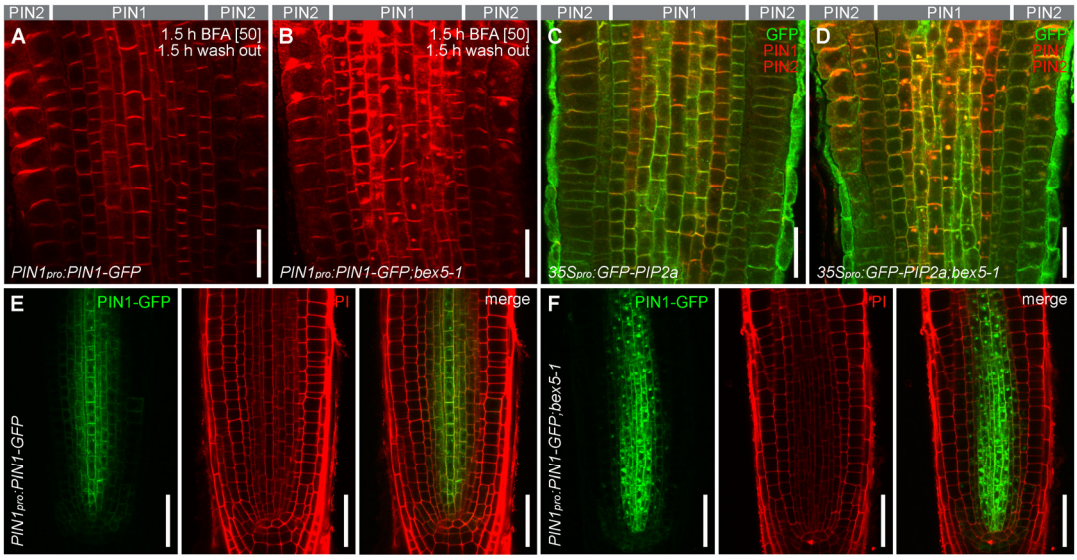

Supplemental Figure 2. *bex5* Is Defective in Exocytosis and Transcytosis of PM Proteins.
(A) to **(D)** Immunolocalizations show abnormal intracellular accumulation of PIN1 (red color in the vasculature cells) (**[A]** to **[D]**), PIN2 (red color in the epidermal and cortex cells) (**[A]** to **[D]**) and GFP-PIP2a (green color throughout the root) (**[C]** and **[D]**) in the *PIN1$_{pro}$:PIN1-GFP;bex5-1* **(B)** and *35S$_{pro}$:GFP-PIP2a;bex5-1* **(D)** lines treated for 1.5-h with 50 µM BFA followed by a 1.5-h wash out in liquid MS medium. In contrast, no or very little accumulation of these proteins could be observed in the *PIN1$_{pro}$:PIN1-GFP* **(A)** or *35S$_{pro}$:GFP-PIP2a* **(C)** lines.
(E) and **(F)** Transcytosis of PIN1-GFP is defective in the *bex5-1*. Wild-type seedlings treated for 16-h with 50 µM BFA show no intracellular accumulation of PIN1-GFP into BFA bodies **(E)**. In contrast, *bex5-1* shows pronounced intracellular PIN1-GFP accumulation **(F)**. Short PI staining (red) shows that long BFA treatment does not interfere with cell viability.
Scale bars are 20 µm **(A)** to **(D)** and 40 µm **(E)** and **(F)**.

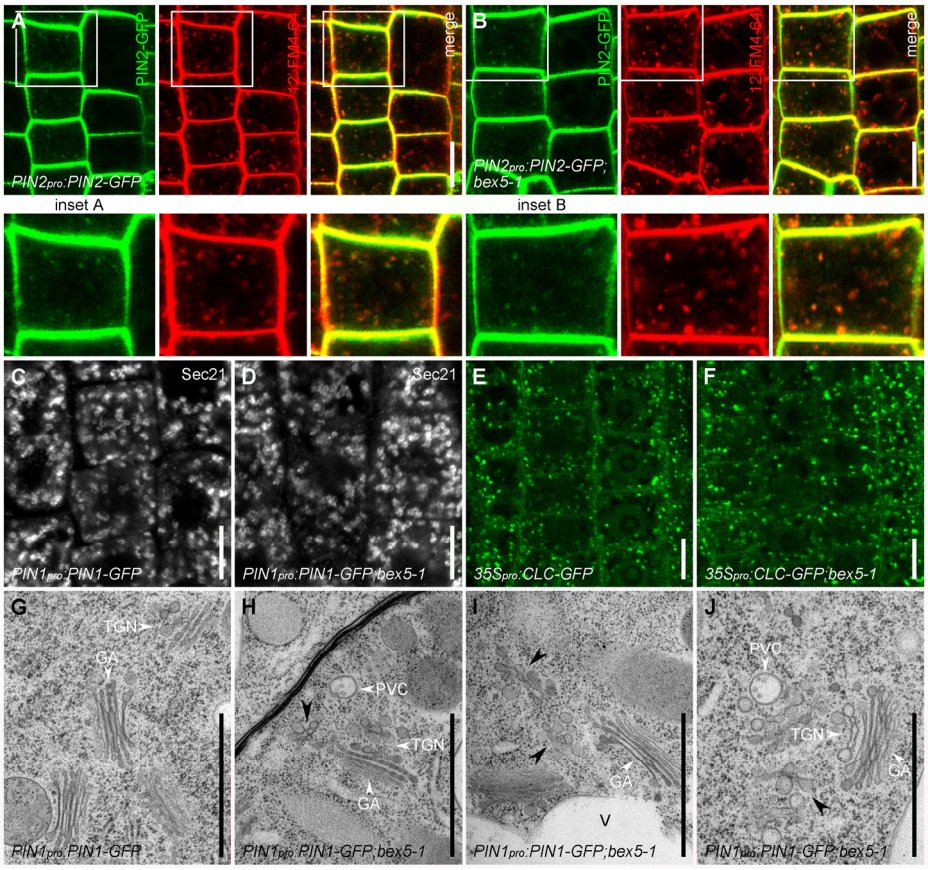

Supplemental Figure 3. *bex5* Shows Abnormal Endosomal Compartments.
(A) and **(B)** PIN2-GFP (green) and FM4-64 (red; 2 µM) label slightly larger endosomal compartments in the *bex5-1* epidermal cells **(B)** as compared to the control **(A)**. Insets represent enlargements of the boxed regions from the corresponding panels.
(C) and **(D)** Immunolocalization of Sec21 in *PIN1$_{pro}$:PIN1-GFP* **(C)** and *PIN1$_{pro}$:PIN1-GFP;bex5-1* **(D)** show that Golgi morphology is not affected in the *bex5-1* mutant.
(E) and **(F)** Live imaging of CLC-GFP localization in wild-type **(E)** and *bex5-1* mutant **(F)**.
(G) to **(J)** *PIN1$_{pro}$:PIN1-GFP* **(G)** and *PIN1$_{pro}$:PIN1-GFP;bex5-1* (**[H]** to **[J]**) cell ultrastructure reveals that *bex5-1* mutant has abnormally fused, shaped and sized vesicles, mainly localized close to one side of the GA-TGN/EE complex. The black arrowheads indicate the abnormal clusters of vesicles in the *bex5-1* mutant.
PVC, prevacuolar compartment. Scale bars are 10 µm **(A)** to **(F)** and 1 µm **(G)** to **(J)**.

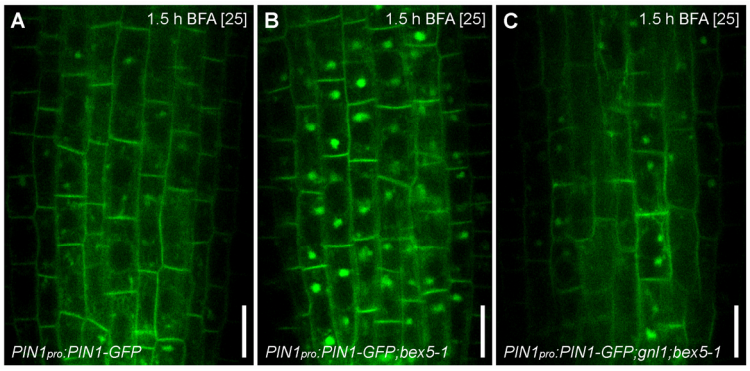

Supplemental Figure 4. *gnl1* Is Epistatic to *bex5*.
(A) to **(C)** Live imaging of PIN1-GFP in the vasculature of wild-type **(A)**, *bex5-1* **(B)** and *gnl1;bex5-1* **(C)** roots treated for 1.5-h with 25 µM BFA. Note that *gnl1* mutation reduces the abnormal BFA-induced PIN1-GFP intracellular agglomeration in the *bex5-1* mutant **(C)**.
Scale bars are 10 µm.

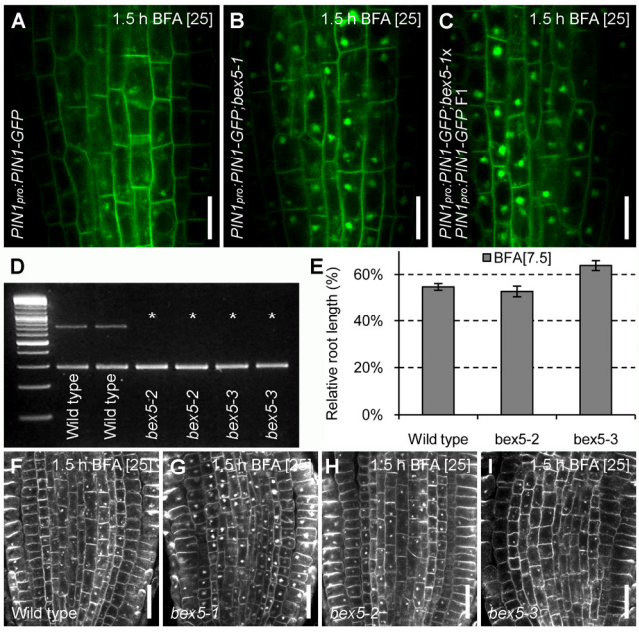

Supplemental Figure 5. *bex5* Is a Dominant RabA1b Mutant.
(A) to **(C)** Live imaging of PIN1-GFP in the vasculature of *PIN1$_{pro}$:PIN1-GFP;bex5-1* **(B)** and *PIN1$_{pro}$:PIN1-GFP;bex5-1* crossed with *PIN1$_{pro}$:PIN1-GFP* and analyzed in the F1 generation **(C)** show similar subcellular sensitivity to a 1.5-h treatment with 25 µM BFA. In contrast, *PIN1$_{pro}$:PIN1-GFP* **(A)** shows reduced intracellular PIN1-GFP accumulation into BFA bodies.
(D) *bex5-2* and *bex5-3* mutants are complete knockouts (asterisk), as indicated by RT-PCR. Tubulin was used as control (lower band).
(E) Five-day-old *bex5-2* and *bex5-3* mutants do not show hypersensitivity to the BFA-mediated inhibition of root growth (n = 60).
(F) to **(I)** Immunolocalization of PIN1 and PIN2 in wild-type **(F)**, *bex5-1* **(G)**, *bex5-2* **(H)** and *bex5-3* **(I)** seedlings treated for 1.5-h with 25 µM BFA. BFA-induced accumulation of PIN1 and PIN2 in *bex5-2* and *bex5-3* is reduced in comparison with their accumulation in *bex5-1*.
Scale bars are 10 µm **(A)** to **(C)** and 20 µm **(F)** to **(I)**. Error bars represent SE.

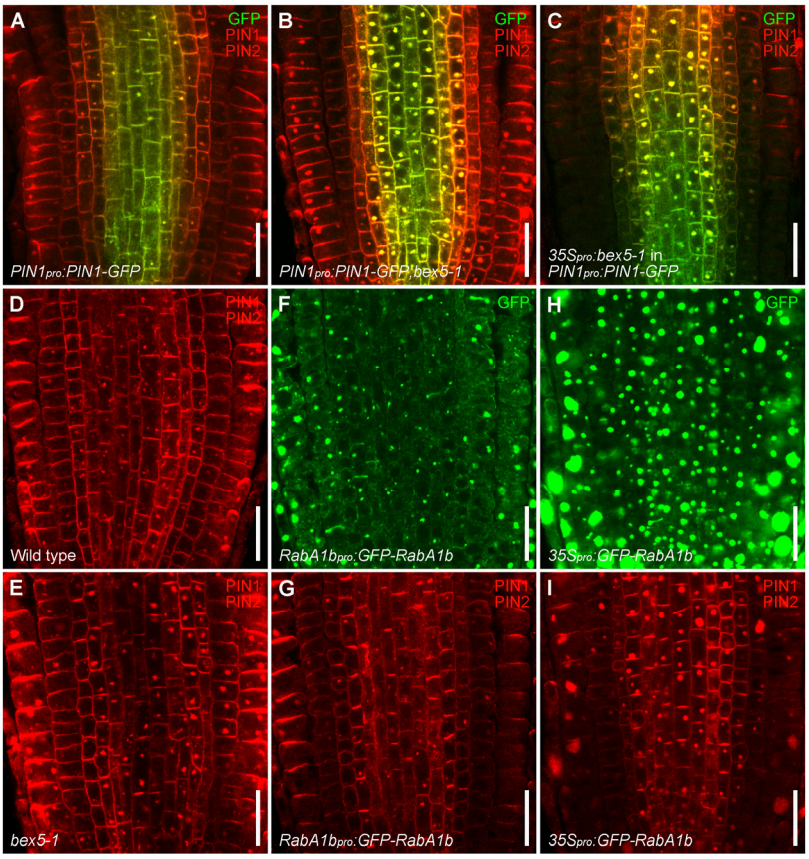

Supplemental Figure 6. *BEX5* Encodes *RabA1b*.
(A) to **(I)** Immunolocalization of PIN1 (red color in the vasculature) and PIN2 (red color in the epidermal and cortex cells) in *PIN1$_{pro}$:PIN1-GFP* **(A)**, *PIN1$_{pro}$:PIN1-GFP;bex5-1* **(B)**, *PIN1$_{pro}$:PIN1-GFP;35S$_{pro}$:bex5-1* **(C)**, wild-type **(D)**, *bex5-1* **(E)**, *RabA1b$_{pro}$:GFP-RabA1b* WT **(G)** and *35S$_{pro}$:GFP-RabA1b* WT **(I)** seedlings treated for 1.5-h with 25 µM BFA show that *PIN1$_{pro}$:PIN1-GFP;35S$_{pro}$:bex5-1* **(C)**, and *35S$_{pro}$:GFP-RabA1b* WT **(I)** display similar BFA-induced abnormal accumulation of PIN1 and PIN2 as *PIN1$_{pro}$:PIN1-GFP;bex5-1* **(B)** or *bex5-1* **(E)**, respectively. Immunolocalization of PIN1-GFP (green color in the vasculature) is shown in *PIN1$_{pro}$:PIN1-GFP* **(A)**, *PIN1$_{pro}$:PIN1-GFP;bex5-1* **(B)** and *PIN1$_{pro}$:PIN1-GFP;35S$_{pro}$:bex5-1* **(C)**. Immunolocalization of *GFP-RabA1b* WT is shown for *RabA1b$_{pro}$:GFP-RabA1b* WT **(F)** and *35S$_{pro}$:GFP-RabA1b* WT **(H)**.
Scale bars are 20 µm.

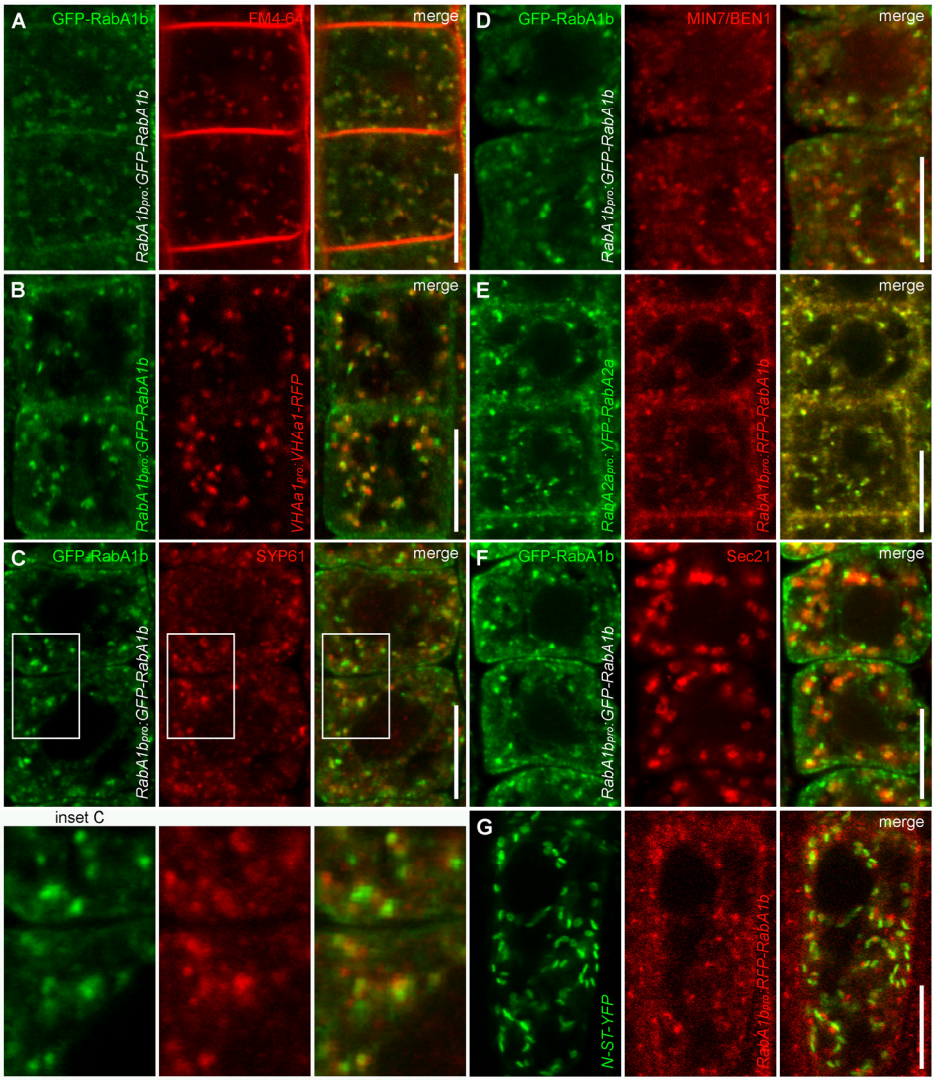

Supplemental Figure 7. BEX5 Localizes at a TGN/EE Compartment.
(A) and **(B)** Live imaging of *RabA1b$_{pro}$:GFP-RabA1b* stained with FM4-64 (2 µM; red) **(A)** or crossed with *VHAa1$_{pro}$:VHAa1-RFP* (red) and analyzed in F1 generation **(B)** shows that GFP-RabA1b (green) partly colocalizes (merge; yellow) with both markers in the root.
(C) and **(D)** Immunolocalizations show that GFP-RabA1b (green) partly colocalizes (merge; yellow) with SYP61 (red) **(C)** or MIN7/BEN1 (red) **(D)**. Insets represent magnifications of the boxed regions from the corresponding panels.
(E) YFP-RabA2a (green) shows complete colocalization with RFP-RabA1b (red) in a *RabA2a$_{pro}$:YFP-RabA2a;RabA1b$_{pro}$:RFP-RabA1b* F1 generation cross.
(F) and **(G)** GFP-RabA1b (green) **(F)** or RFP-RabA1b (red) **(G)** are distinct of Sec21 (red) **(F)** and N-ST-YFP (green) **(G)** although they are often close together. Note that the predominant punctuate shape of RabA1 endosomes is different than that of Sec21 and N-ST endosomes. Immunolocalization **(F)**. Live imaging of *35S$_{pro}$:N-ST-YFP;RabA1b$_{pro}$:RFP-RabA1b* F1 cross **(G)**.
Scale bars are 10 µm.